**Wiesław Barnat,
Dariusz Sokołowski,
Roman Gieleta**

**Department of Mechanics
and Applied Computer Science,
Faculty of Mechanical Engineering,
Military University of Technology,**
ul. Kaliskiego 2, 00-908 Warsaw, Poland
E-mail: dsokolowski@wat.edu.pl

Numerical and Experimental Research on Stab Resistance of a Body Armour Package

Abstract
In this paper the issue of the stab resistance of a ballistic package is addressed. Emphasis was placed on this issue because most modern vests are designed to meet the threat posed by firearms only. Neglect of protection against melee attacks was also observed. Thus there is a need to develop research methodology for this area, also because it is a valid and necessary problem to be addressed in a modern, developed society. The aim of this study was to create a numerical model which simulated the phenomenon of ballistic package penetration by a test blade. The specification of the test blade was taken from NIJ Standard-0115.00. During the research, stab resistance tests on dry Twaron T750 fabric was carried out on a drop test machine. The test was filmed with a Phantom V12 high-speed camera. A numerical model of the fabric architecture was prepared using commercial LS-DYNA software. The numerical model represents the whole research area according to NIJ Standard-0115.00. As backing material, ROMA 1° ballistic clay was used.

Key words: *numerical model, dry fabric, aramid fabric, stab resistance, body armour.*

Introduction

In this paper the issue of a knife proof ballistic package is addressed. Emphasis was placed on this issue because most modern vests are designed to meet the threat posed by firearms only. Neglect of protection against melee attacks was also observed. There is thus a need to develop research methodology in this area, because it is a valid and necessary problem to be addressed in a modern, developed society [1, 2].

The number of firearms on Polish streets is not so large compared to, for example, the United States. Polish legislation effectively takes care of restricting access to firearms for persons with inappropriate predispositions. As for melee weapons, the case is diametrically different as access to melee weapons is unlimited. Each kitchen has a whole arsenal of objects that can be used as a weapon against officers of the uniformed services.

In this paper the problem of the numerical modelling of aramid dry Twaron T750 fabric has been raised. This fabric is a special-purpose material used in the manufacture of bulletproof vests. Twaron T750 fabric is characterised by a high dense weave. In order to achieve a reliable model of real fabric, a drop test of six samples made of Twaron T750 fabric on a drop column was made. These studies were used to create the most precise numerical model as possible by means of commercial software LS-DYNA.

The rapid development of computational techniques has allowed to create a more detailed description of the structures of dry fabrics. Yet in the not so distant past, the dry fabric of the bullet impact test was modelled in the form of an averaged material continuum, which was built using a membrane or shell elements. With the arrival of more and more powerful computational units on the market, there appeared options for modelling of fabric weave architecture and bundle thickness. This kind of modelling allows to grasp the phenomena of contact between bundles of roving, enabling to represent the phenomena of movement between bundles. In the literature there are three ways of modelling roving bundles in fabric architecture. The first is to model the bundles in the form of flat elements (with specified thickness, so called 2D) [4].

The second approach is to model the bundles using three-dimensional elements [3, 5 - 7]. The third is by hybrid modeling. The most cost-effective computational method is, of course, the use of 2D components.

This type of analysis is used in cases where the fabric is loaded in the plane. Despite the large approximations, this kind of modelling is fully effective and efficient. In this paper the problem of modelling special fabrics was considered using 2D elements. 3D modelling of roving bundles should be used to model the fabric, which is loaded perpendicular to the plane, making such models very expensive computationally. So far, in modelling bundles, authors such as Nilakantan or Barauskas used two 3D elements for the thickness of the bundle, which in the modelling of other phenomena is rather unacceptable.

In the literature available there is a lack of examples of the validation of numerical models with experimentation in case studies using dry fabrics. This article will present the validation of a numerical model fort Twaron T750 fabric with experimental results.

Physical description of existing phenomena

The basis for the phenomenon is the NIJ Standard-0115.00, which describes a research method for the stab resistance of ballistic packages. According to this standard, the free falling sabot system, which has the kinetic energy required arising from the standard, hits the ballistic package lying motionless on a deformable surface.

Described in the paper, the phenomenon is complex because there are many interactions between the elements. Besides the structure of individual elements is not trivial. The most complicated system in the experiment is testing a ballistic package which consists of 35 layers of Twaron T750 fabric. Each layer of fabric is composed of hundreds of roving bundles, and each roving bundle consists of about 2,000 aramid fibres with a thickness of about 15 μm. Between all of the above- mentioned parts are contact phenomena, which introduce a strong nonlinearity in the system. Besides this the same geometry of roving bundles is also complicated. At this point, attention should be paid to the fact that between aramid fibres there is air, which introduces damping to the system, which is difficult to determine. Damping is an important element in dynamic issues. Between the same roving bundles there is air-filled emptiness.

Barnat W, Sokołowski D, Gieleta R. Numerical and Experimental Research on Stab Resistance of a Body Armour Package.
FIBRES & TEXTILES in Eastern Europe 2014; 22, 6(108): 90-96.

Another element constituting a part of the system is the sabot set, which consists of four parts connected with unilateral nodes (***Figure 1***). One of the parts constituting the damping element is made of low density polyurethane foam, which introduces, apart from damping, a very strong non-linearity to the system, arising from the character of the stress strain function.

Figure 2 shows a test knife, which is a key element of the model. Its geometry strongly influences the course of the phenomenon. Its asymmetrical design results in an uneven load ballistic contribution and produces the highest energy density per blade; at the same time the blade thickness prevents buckling. This causes the greatest threat of ballistic contribution. The knife presented in ***Figure 2*** during impact slides roving bundles apart, simultaneously cutting aramid fibres which are in contact with it.

The final element of the system is a backing material made of ballistic clay ROMA no. 1, which has a high coefficient of damping and energy dissipation, low Young's modulus and ease of plastic flow. In the system clay symbolises the human body.

Figure 3 shows a simplified diagram of the physical phenomenon occurring in a system with a falling sabot set, ballistic package and clay representing the human body. The figure presents the structure of the system and the relevant physical quantities.

The diagram of the system presented abovein ***Figure 3*** can be easily described by analytical methods using general formulas [12, 13].

$$dE = d'L \tag{1}$$

The law of variation of the kinetic energy of the system (1) can be written for each system component in the form of ***Equation 2***.

$$d\left(\frac{1}{2}m_i v_i^2\right) = \vec{F}_i d\vec{r}_i + \vec{W}_i d\vec{r}_i + \\ + \vec{R}_i d\vec{r}_i, (i = 1, \dots, n) \tag{2}$$

where:
m_i - mass point *i*,
$\vec{F}_i$ - the resultant active forces acting on point *i*,
$\vec{R}_i$ - the resultant reaction forces acting on point *i*,

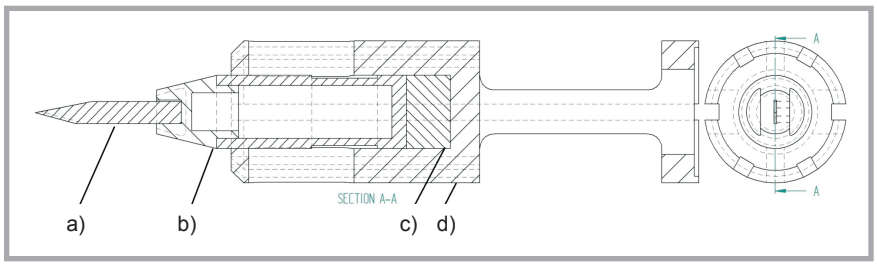

Figure 1. *Sabot cross-section with mounted test knife: a) test knife, b) knife handle, c) damping element made with low density foam, d) nylon sabot.*

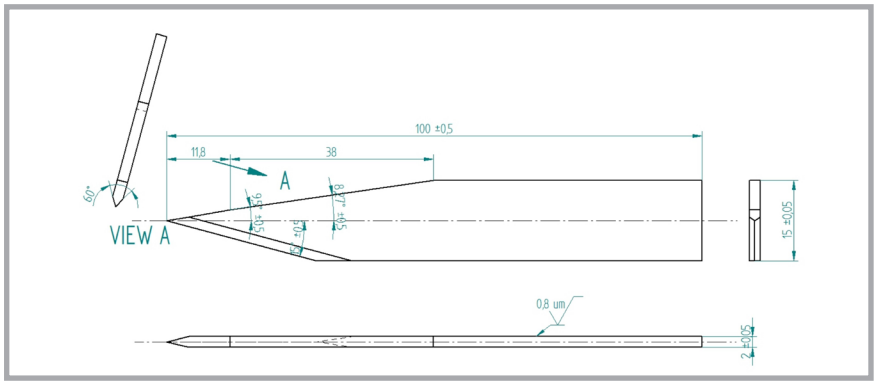

Figure 2. *P1 test knife according to NIJ Standard-0115.00.*

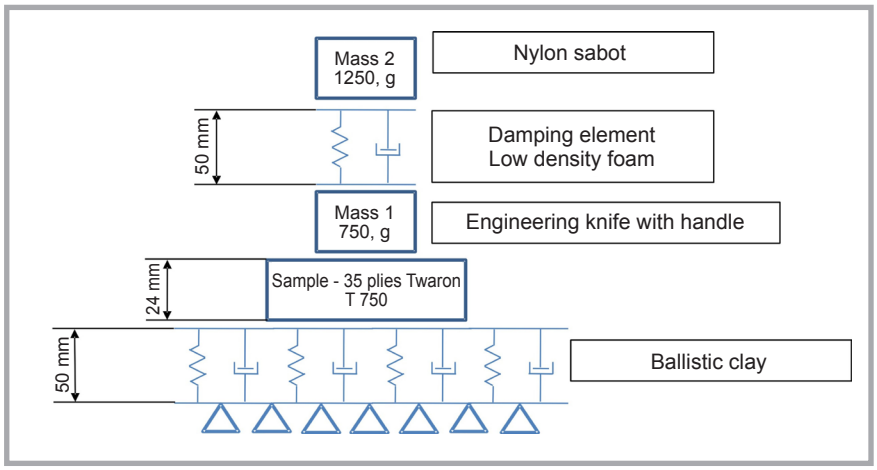

Figure 3. *Simplified diagram of the physical phenomenon.*

$\vec{W}_i$ - the resultant internal forces acting on point *i*,

$$d\left(\frac{1}{2}\sum_{i=1}^{n} m_i v_i^2\right) = \sum_{i=1}^{n}(\vec{F}_i d\vec{r}_i + \\ + \vec{W}_i d\vec{r}_i + \vec{R}_i d\vec{r}_i) \tag{3}$$

After summing the *i* elements of the system we can formulate formula (3) which describes the change in energy of the entire system.

$$dE = d'L_F + d'L_W + d'L_R \tag{4}$$

A problem occurs at the time of the determinate of internal forces in the elements of the system and the reaction between the elements of the system, due to strong nonlinearities in the analytical process of determining these values. Hence it was decided to use approximate methods, namely numerical. For the calculation finite element method was chosen with explicit integration equations of motion over time.

Algorithm explicit integration of equations of motion using ***Equation 5*** for known configuration at the time of t_k is

$$M\ddot{r} + C\dot{r} = F_k^{ext} - F_k^{int} \tag{5}$$

From ***Equation 5*** there is defined a solution for the next moment of time - ***Equation 6***.

$$t_{k+1} = t_k + \Delta t_{k+1} \tag{6}$$

Table 1. *Manufacturer's material card [Teijin Aramid, (2012)].*

Style	Linear density, dtex nom	Twaron-type	Weave	Set, per 10 cm		Set, per inch		Surface mass		Thickness, mm	Minimum breaking strength, N/5 cm × 1.000		Minimum breaking strength, lb/in × 1.000	
	Warp/Weft	Warp/Weft		Warp	Weft	Warp	Weft	g/m²	oz/yd²		Warp	Weft	Warp	Weft
CT T750	3360f2000	2000	Plain	69	69	18	18	460	13.57	0.70	16.5	18.00	1.884	2.056

A typical algorithm explicit integration is the scheme of central differences with a variable step of integration.

$$\ddot{r} = M_D^{-1}(F_k^{ext} - F_k^{int} - C\dot{r}) \quad (7)$$

where:
$M_D = diagM$

Replacement of matrix M, which is a consistent mass matrix from a clustered mass matrix (diagonal), allows the decomposition of the equations of motion, which increases the numerical efficiency of the process.

$$\dot{r}_{k+1/2} = \dot{r}_{k-1/2} + \ddot{r}\Delta t_{k+1/2} \quad (8)$$

$$r_{k+1} = r_k + \dot{r}_{k+1/2}\Delta t_{k+1} \quad (9)$$

where:

$$\Delta t_{k+1/2} = \frac{1}{2}(\Delta t_k + \Delta t_{k+1}) \quad (10)$$

At each time step the following are calculated: acceleration, velocity, and displacement nodes of finite elements (7), (8), (9).

The advantage of explicit integration of equations of motion is the conditional stability of the process, through which there can be resolved issues with strong non-linearity. However, provided that the integration step must be shorter than the threshold step, called the critical step (11), in the model without damping and model (12) with damping, then

$$\Delta t \le \Delta t_{cr} = \frac{2}{\omega_{max}} \quad (11)$$

$$\Delta t_{cr} = \frac{2}{\omega_{max}}(\sqrt{1+\xi^2} - \xi) \quad (12)$$

where:
$\omega_{\max}$ – highest natural frequency of the system
ξ – damping coefficient

Numerical model of phenomenon

The aim of the numerical model was to project the physics of the phenomenon as precisely as possible. The choice of weave shape was modelled based on information from the manufacturer's material card.

The volume share ratio of Kevlar fibres in the bundle was calculated (based theon the material manufacturer card's) at 50% of the bundle. Substitute The *p*'s Young's modulus of the placeholder was determined using the law of mixtures from literature, for the assumed rate of volume [8]. The density of the bundle was reduced to 50% of that of Kevlar.

$$E_{11} = E_W V_W + E_0(1 - V_W) \quad (13)$$

where: E_{11} – Young module in the direction of the bundle, E_W – Young module of Kevlar, V_W – volume ratio, E_0 – matrix Young module (air in this case - taken as equal to zero)

It was decided to model roving bundles using shell elements. Each bundle is an individual object connected only to other ones by contact definition. The following contact definition was used: CONTACT_AUTOMATIC_SURFACE_TO_SURFACE. This kind of impact-contact algorithm the contact segment - a segment, in that element (segment) located on the body of the master searches for the slave nodes, then the whole procedure is carried out vice versa. In the contact card, the variable thickness of the cross-section of the bundle was defined. This approach allowed to control penetration at a constant elasticity of the roving bundles. The model was made based on 2D fully integrated shell elements of constant thickness.

A material model was implemented to describe the bundles: MAT_ORTHOTROPIC_ELASTIC.

The material describes the coupling between the strain tensor Green-St. Venant "ε" and stress tensor Piola-Kirchhoff "S".

$$S = C \cdot E = T^t C_1 \mathrm{T} \cdot \varepsilon \quad (14)$$

where:
T - transform matrix.
C_1 - constitutive matrix.

The material constants that were used in the card of the material were a Young module equal to 57 GPa, a Poisson ratio of 0.001, a shear modulus of 0.1 GPa and principal stress equal to 1550 MPa in the MAT_ADD_EROSION card. Through the use of a very small number of Poisson, stresses could separate in the directions perpendicular to the bundle direction.

The backing base was made of ROMA 1o ballistic clay, modelled using MAT_POWER_LAW_PLASTICITY, with material constants from literature [15].

Elastoplastic behavior with isotropic hardening is provided by this model. The yield stress, σ_y, is a function of the plastic strain, obeying the equation:

$$\sigma_y = k\varepsilon^n = k(\varepsilon_{yp} + \overline{\varepsilon}^p)^n \quad (15)$$

where ε_{yp} is the elastic strain to yield, ε^p the effective plastic strain (logarithmic), and n is the hardening exponent.

The Young module is equal to 4 MPa, the Poisson ratio 0.4, the strength coefficient 0.244 MPa and the hardening exponent 0.093 (***Figure 5.a***). The delay element, made of low density polyethylene foam, was modelled using MAT_LOW_DENSITY_FOAM with a stress strain curve form literature [16].

The model uses tabular input for the load curve, where the nominal load is defined as the function elongation ε_i, which is defined as principal stretches λ_i

$$\varepsilon_i = \lambda_i - 1 \quad (16)$$

The stretches are found by resolving the eigen values of the left stretch tensor, V_{ij}, which is obtained by polar decomposition of the deformation gradient matrix F_{ij}.

$$F_{ij} = R_{ik}U_{kj} = V_{ik}R_{kj} \quad (17)$$

Numerical test results

The aim of the numerical research was to present displacement, velocity and acceleration curves.

During the numerical research special emphasis was placed on two things: first the value of the final displacement recorded for the test knife, and second the matching course of curves like displacement, velocity and acceleration.

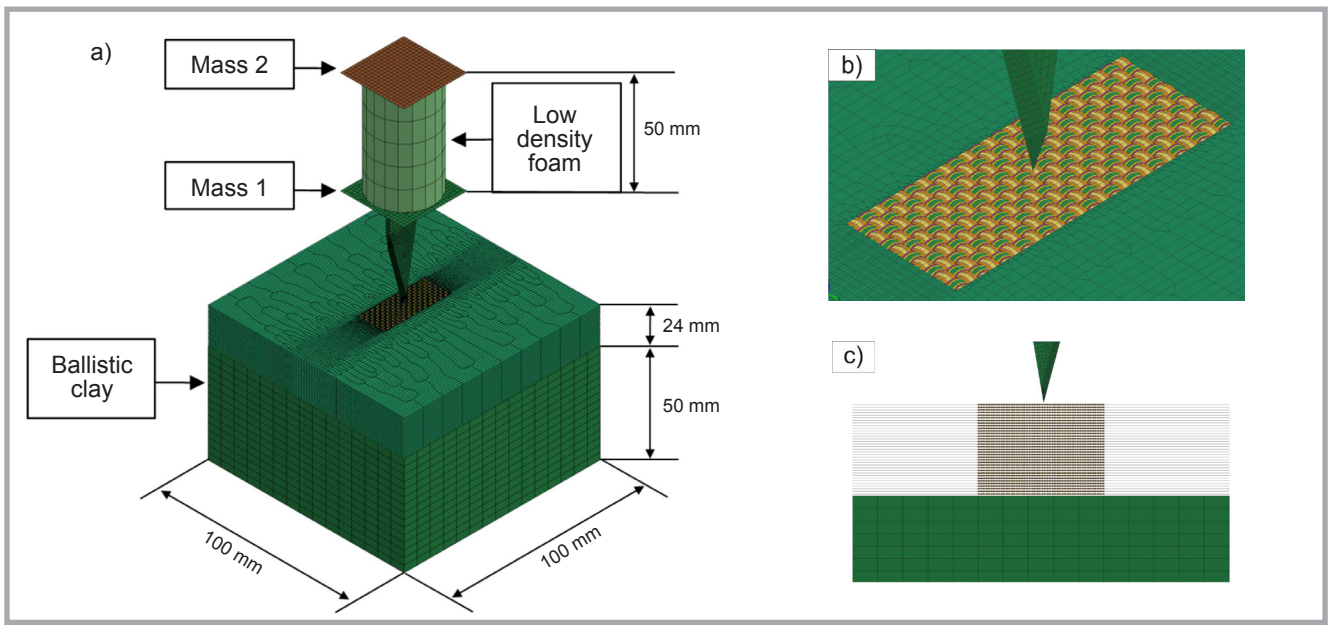

Figure 4. *a) Izoparametric view of numerical model, b) zoom of accurate region, c) side view of numerical model.*

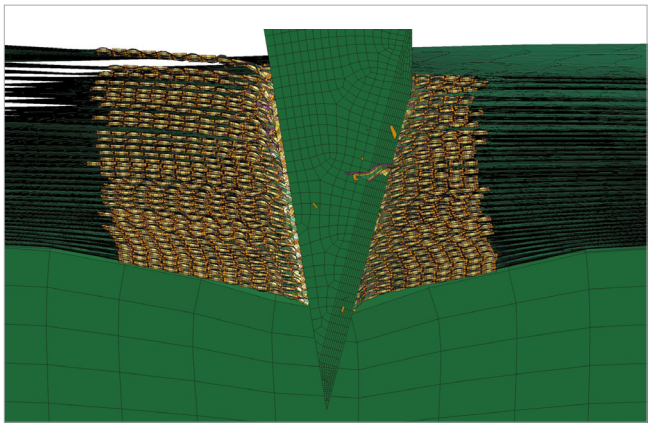

Figure 5. *Cross section of numerical model for time t = 30 ms.*

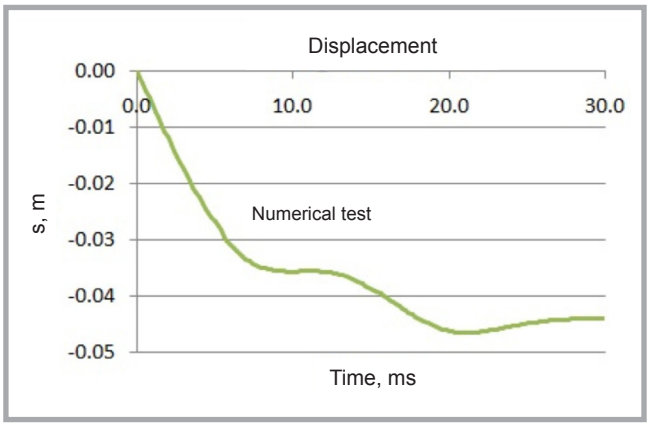

Figure 6. *Comparison of displacements.*

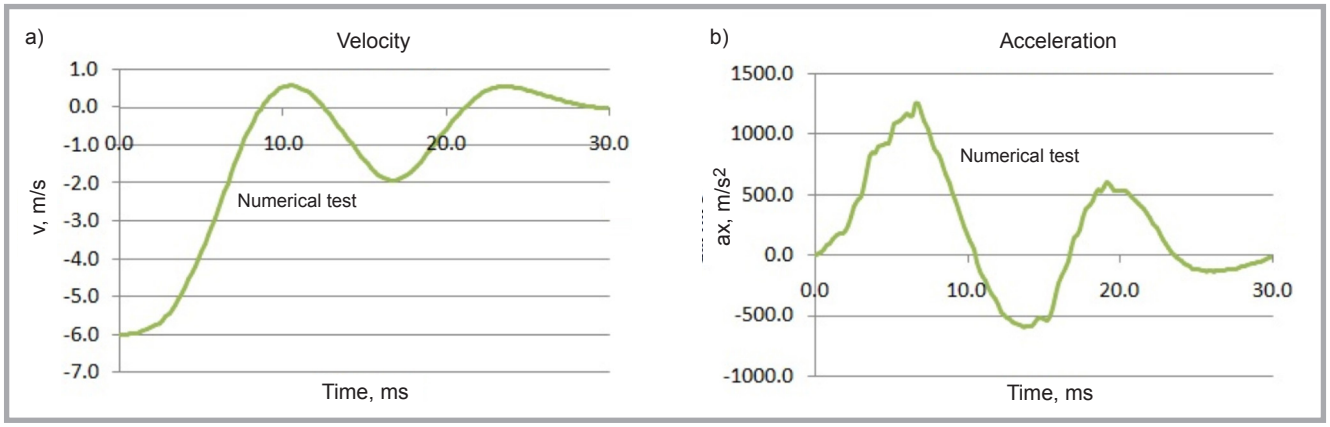

Figure 7. *a) comparison of velocities, b) comparison of acceleration.*

Figure 5 shows the cross section of the numerical model at the final moment of time equal to 30 ms. with the displacement at that moment being equal to 44.2 mm. The maximal penetration was equal to 14,6 mm, different from that measured in experimental research. This is caused by the fabric not being drawn into the clay, as was in the experimental research.

Figure 6 shows the displacement of the knife test. ***Figures 7.a*** and ***7.b*** show the velocity and acceleration, respectively, of the knife test. The charts are continuous, with no observable abrupt changes in the course of the curves, which means that the contact model worked correctly from the first time. In other words, the contact was properly configured.

Figure 8. *Drop column.*

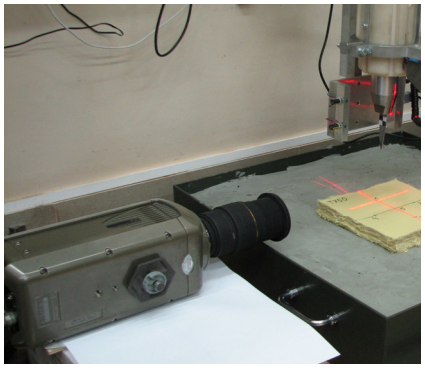

Figure 9. *Test area with placed sample.*

During the eroding of elements, subsequent elements smoothly came into contact with the knife, constantly propping it and dissipating energy to work against the forces of elasticity of the material of the package and eroding elements.

The knife in the initial moments slightly moved the roving bundle apart, and then after exceeding the limit adopted principal stress, tearing the bundles sequentially. After tearing them, the knife pulled them slightly into the ballistic package. Contact force between the knife and fabrics increased with the knife sinking into the ballistic package.

Experimental tests

This part of article presents an experimental approach to the phenomena. ***Figure 8*** shows a drop column with time gate equipment. Inside the drop column a sabot is installed according to NIJ Standard-0115.00. The sabot consists of a test knife with a handle, a delay element made of low density polyethylene foam and a Nylon sabot.

Figure 9 shows a banking base made of Roma 1° ballistic clay (in the black box), a time gate and Phantom V12 high speed camera. A test sample made of 35 plies of Twaron T750 dry aramid fabric was placed on the ballistic clay.

Figure 10 shows a top view of the test sample. Predicted places of knife hits are marked by numbers. Distances between hits are according to NIJ Standard-0115.00 and equal to 50.8 mm (2 in).

Figure 10. *Test sample with marked places for hits.*

Table 2. *Results of experimental research.*

Test	Kinetic energy, J	Penetration, mm	Velocity, m/s
1	36.26	9.56	5.958
2	36.20	7.90	5.953
3	36.15	12.30	5.949
4	36.20	10.70	5.953
5	36.25	11.92	5.957

Experimental test results

Tests on the drop column were made in a laboratory for testing KMiIS MUT. Tests were filmed by a PHANTOM V12 high speed camera (USA) with a frequency of 5000 frames/s. The test knife was marked by a black and white checkerboard. Thanks to the marker and Tema 3.3 software it was possible to accurately record such quantities like displacement, velocity and acceleration for a knife with a handle.

As a result of the experiment, 5 movies were recorded using a high speed cam-

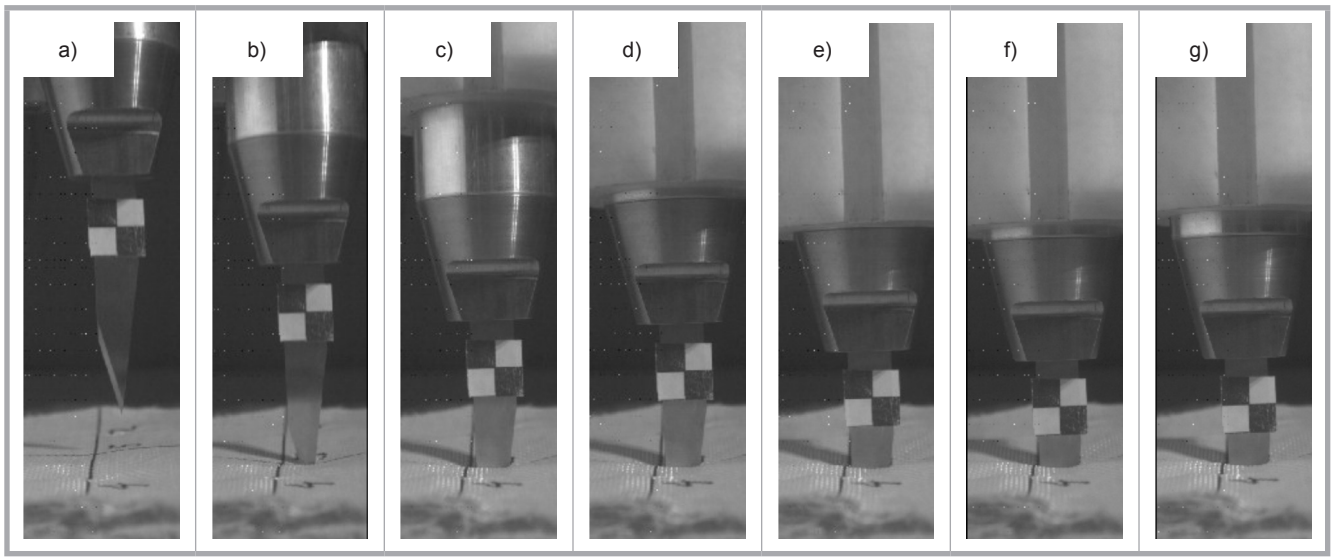

Figure 11. *Frames recorded by Phantom V12 camera: a) t = 190 ms, b) t = 186.8 ms, c) t = 184.4 ms, d) t = 175 ms, e) t = 170 ms, f) t = 165 ms, g) t = 160 ms.*

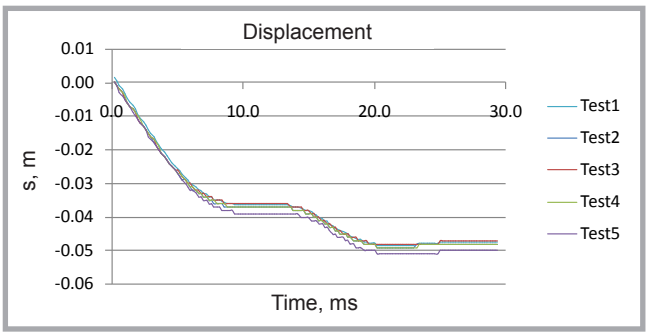

Figure 12. *Displacements of test knife for each test.*

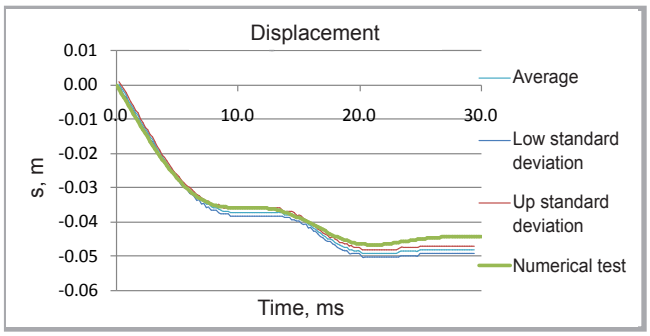

Figure 14. *Comparison of displacements.*

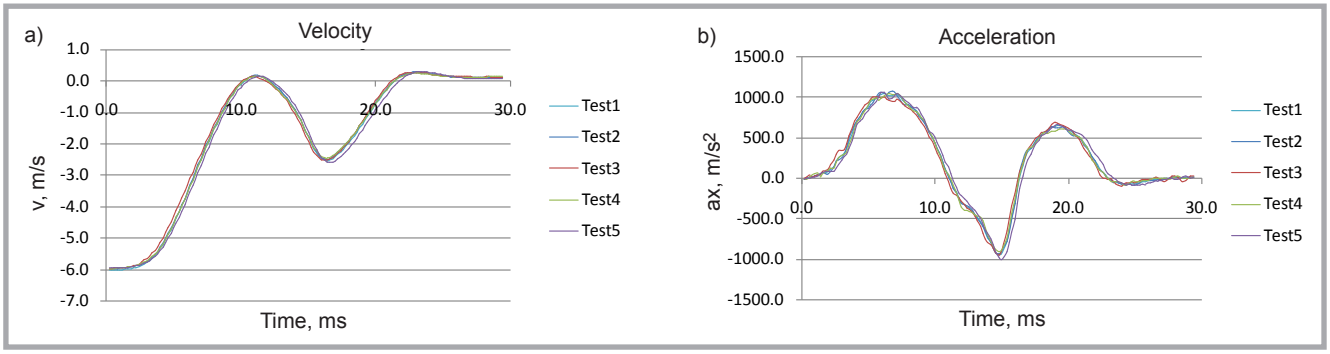

Figure 13. *a) Velocity of knife, b) acceleration of knife.*

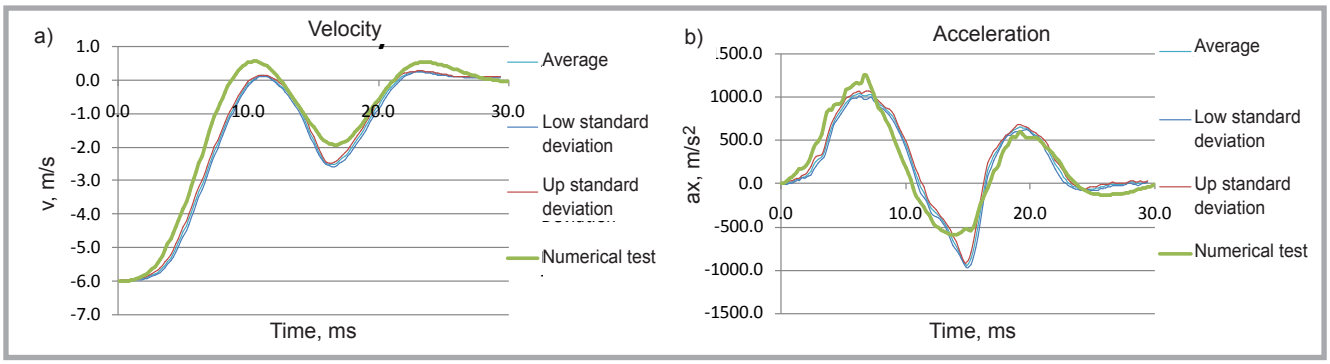

Figure 15. *a) comparison of velocities, b) comparison of acceleration.*

era - PHANTOM V12. The movies were post-processed in Tema 3.3 software. As a result of post-processing, the graphs showed displacement, see ***Figure 12***, the velocity in ***Figure 13.a*** and acceleration in ***Figure 13.b***. In ***Figure 12*** two areas can be seen where the displacement increases and two areas where the increment of displacement is stopped. This effect is clearly visible in ***Figure 13.a***, caused by the construction of the sabot, which consisted of two independent masses (mass 1 – knife with a handle - 750 g and mass 2 – nylon sabot - 1250 g), between which a delay element made of low density polyethylene foam was located. When mass 1 dissipates, its own kinetic energy is loaded by the still moving mass 2, causing an increase in the velocity of mass 1. ***Figure 13.b*** shows the acceleration for mass 1. Two impulses of acceleration can be seen, which are equal to the quantity but with an opposite sign. The first impulse is caused by the impact of the knife and handle with the fabric, and the second by the moving of mass 2.

Conclusions

This paper is an example of an effective connection experimental and numerical research, thanks to which a faithful description of the complex physical phenomenon was made.

Figure 14 shows a comparison between the displacement obtained from the experimental and numerical tests. Both curves have a similar shape but their ends slightly differ. ***Figures 15.a*** and ***15.b*** show the velocity and acceleration. Differences between the average experimental curves and numerical ones are bigger, caused by a discrepancy between the material date culled from literature for clay and foam and that for clay and foam used in the experiment. In future additional studies are required in order to determinate material properties for foam and clay which will be used in the experiment. The modelling of these materials is difficult because of the high non-linear behaviour.

It has been proven that 35 plies of dry aramid fabric is able to stop a knife blade, but body armour consisting of 35 plies has more than enough weight to carry. For this reason it is important to find

another material and configuration to reduce body armour weight.

Editorial note

The problem described by this article was partly presented (but not published) on the 13th International Conference 'The Latest Trends in the Construction and Applications of Ballistic Armour", 4-5 september 2013, Lodz, Poland.

Acknowledgement

The project is financed by the National Centre for Research and Development Programme in the path INNOTECH in INNOTECH-K2/ IN2/56/182840/NCBR/13.

References

1. Johnson A, Bingham AG, Majewski EC. Establishing the performance requirements for stab resistant Additive Manufactured Body Armour (AMBA). In: *The 23rd Annual International Solid Freeform Fabrication (SFF) Symposium*, 2012: 297-306.
2. Horsfall I. *Stab Resistant Body Armour*. Cranfield University, Engineering Systems Department Submitted For The Award Of PhD, 2000.
3. Barauskas R. Multi-Scale Modelling of Textile Structures in Terminal Ballistics. In: *6th European LS-DYNA Users' Conference*, 2007.
4. Ha-Minh C, Imad A, Kanit T, Boussu F. Numerical analysis of a ballistic impact on textile fabric. *International Journal of Mechanical Sciences* 2013; 69: 32–39. DOI: 10.1016/j.ijmecsci.2013.01.014.
5. Nilakantan G, Keefe M, Gillespie JW Jr., Bogetti TA, Adkinson R. A Study of Material and Architectural Effects on the Impact Response of 2D and 3D Dry Textile Composites using LS-DYNA. In: *7th European LS-DYNA Users' Conference*, 2009.
6. Nilakantan G, Keefe M, Gillespie JW Jr., Bogetti TA. Novel Multi-scale Modeling of Woven Fabric Composites for use in Impact Studies. In: *10th European LS-DYNA Users' Conference*, 2008.
7. Nilakantan G, Keefe M, Gillespie JW Jr., Bogetti TA, Adkinson R, Wetzel ED. Using LS-DYNA to Computationally Assess the V0-V100 Impact Response of Flexible Fabrics Through Probabilistic Methods. In: *11th European LS-DYNA Users' Conference*, 2010.
8. Jones RM. *Mechanics of composite materials*. Taylor & Francis Inc., 1999.
9. LS-DYNA, Keyword User Manual, 2007.
10. LS-DYNA, Theory Manual, 2006.
11. Livermore Software Technology Corporation, Modeling of Composites in LS LS-DYNA.
12. Kozłowski R, Krasoń W. Numerical simulations in the study of water crossings on the example of a prototype pontoon bridge. *Mechanik* 2013; 11: 980-981.
13. Krasoń W, Kozłowski R. Dynamic analysis of a multi-mechanism on the example of special floating segments. *Biuletyn WAT* 2013; LXII, 3: 171-194.
14. Teijin Aramid. *Ballistics material handbook*, 2012.
15. Sofuoglu H, Rasty J. Flow behavior of Plasticine used in physical modeling of metal forming processes. *Tribology International* 2000; 33: 523–529.
16. Ouellet S, Cronin D, Worswick M. Compressive response of polymeric foams under quasi-static, medium and high strain rate conditions. *Polymer Testing* 2006; 25: 731–743.

Received 16.01.2014 Reviewed 31.03.2014